

PLASMA ELECTROLYTIC OXIDATION (PEO) COATINGS ON A ZIRCONIUM ALLOY FOR IMPROVED WEAR AND CORROSION RESISTANCE

Y. Chen¹, X. Nie², D. O. Northwood³

^{1,2,3}Department of Mechanical, Automotive, & Materials Engineering, University of Windsor, Windsor, ON, Canada, N9B 3P4

Abstract

Zr oxide coatings were deposited using plasma electrolytic oxidation (PEO) on Zr-2.5wt%Nb alloy, which is currently used for pressure tubes in the CANDU nuclear reactor. The effects of three processing factors: electrolyte concentration, current density, and terminal voltage on the microstructure and property of coatings were systematically investigated. The coating morphology was determined using scanning electron microscopy (SEM). Potentiodynamic polarization corrosion testing was used to exam the corrosion resistance of the coatings in a LiOH aqueous corrosion media. Pin-on-disc wear tests were performed under dry sliding test conditions in air coefficient of friction was calculated according to the tribological test. SEM was also used to characterize the wear tracks on the coatings. According to the research, recommendations are made as to processing parameters for the production of oxide coatings with improved wear and corrosion resistance.

1. Introduction

The Zr-2.5Nb is used in a nuclear reactor have good corrosion resistance and mechanical properties at a high temperature and neutron stability. The recent trends of high fuel burn-up, extended recycle and high PH operation for increasing energy efficiency has led to the need to improve the corrosion resistance of Zr-2.5Nb, which is now used in CANDU[1-3].

Plasma electrolytic oxidation (EPO) is a technique by which a ceramic coating can be grown in-situ on Al, Ti, Mg and many other light metals[4]. The coatings prepared by the PEO technique are reported to have fine properties like corrosion resistance, anti-abrasion property or decorative property and so on and the promising application prospect in many fields. It has been developed as an environmentally friendly surface engineering technique for wear and corrosion protection of Zr alloys. In PEO technology, sparks or arc plasma micro-discharges in an aqueous solution are used to ionize gaseous media from the solution with the result that complex compounds are synthesized on the metal surface by the plasma-chemical interactions. These technologies were used, first of all, for the surface hardening and enhancement of the corrosion resistance of aluminum[5] and, recently, magnesium and titanium alloys[6]. Few instances of research of PEO technique to Zr alloys in the alkaline solutions [7, 8].

In this study, we have utilized the EPO technique to deposit Zr-Si-O ceramic coatings with a high adhesion, hardness and thickness on Zr-2.5Nb substrates using an pulsed DC power supply in a silicate solution. Two groups (group A and group B) of Zr specimens were oxidized in Na₂SiO₃ and KOH

solutions with different ratios (8g/L:8 g/L and 8 g/L:0.8 g/L). In each group, two current densities (0.05 A/cm² and 0.15 A/cm²) and two terminal voltages (350V and 400V) were used to make different coatings. Tribological and wear behaviours before and after corrosion were investigated.

2. Experiment details

Square coupons with dimensions of 15X13X4mm³ were cut from commercial Zr-2.5Nb alloy and used as the substrates. All the coupons were first flatted with abrasive papers from 120-4000 degree and polished by 5 micron and 1micron micropolish alumina and cleaned to obtain a uniform surface roughness of Ra=0.1±0.02µm.

A pulsed DC power supply with frequency of 2000Hz was used to produce the EPO coatings. An alkali-silicate solution (Na₂SiO₃ with KOH) was used as the electrolyte. A constant current density of 0.15A/cm² or 0.25A/cm² was used during the coating process, and the voltage was increased gradually with process time so as to maintain the preset current density as the coating thickness gradually increased. The voltage variation vs. treatment time was recorded for both groups. Four samples for each group were treated at different voltage ranges and current densities. The electrolyte temperature was controlled to remain lower than 60°C.

Potentiodynamic polarization tests were carried out for both uncoated and coated samples at room temperature (20 °C) using a SP-150 potentiostat/galvanostat produced by Bio-Logic with Corrware software. Potentiodynamic polarization measurements were made in a conventional three-electrode cell using a Ag/AgCl/sat KCL electrode as the reference electrode, and a platinum rod as a counter electrode. The measurements were carried out in 4.8 wt.% (0.4mol/L) LiOH solution, which was chosen for its great enhancement to the corrosion rate of Zr alloys[9]. The exposure area of the sample was 1 cm². After the electrochemical testing system was stable, scans were conducted at a rate of 1mV/s from -0.5V versus open circuit potential (OCP) in a more noble direction up to 2V versus the reference electrode. Potentiodynamic polarization curves of the tested samples were obtained and corrosion rates were determined for comparison.

The tribological properties were tested by means of a pin-on-disc tribometer (CSM high temperature tribometer) at room temperature (20 °C) and ~30% humidity. Tribological testing on the uncoated substrate and coated samples was performed under 1N normal load with sliding distance of 30m and 2 N normal load with sliding distance of 250m, at a 0.1m/s sliding speed Alumina Oxide balls (5.5mm in diameter) were used as the counterface material. A circular mode was chosen with a 4mm diameter wear trace. A SJ-201Pstylus surface profilometer was used for surface roughness (Ra) measurements both before and after corrosion testing.

Scanning electron microscopy (SEM) with energy dispersive X-ray analysis system (EDS) was employed for the study of the coating surface morphology and composition. Cross-sectional SEM micrographs at different magnifications were also taken to study the thickness of the coatings.

3. Result and discussion

The process parameters as well as surface roughness (Ra) are listed in Table 1 and the Ra vs process time data of all the eight coatings were plotted in Figure 1.

Table1 Process parameters and average roughness of coatings

Samples	Electrolyte ratio (Na ₂ SiO ₃ :KOH)	Current density (A/cm ²)	Terminal voltage (V)	Process time(min)	Average surface roughness(Ra μm)	
Group A	8g/L:8 g/L	a1	0.15	350	1.56	0.48
		a2	0.15	400	2.2	0.82
		a3	0.25	350	0.35	0.54
		a4	0.25	400	0.4	1.43
Group B	8 g/L:0.8 g/L	b1	0.15	350	2.55	2.89
		b2	0.15	400	2.46	2.49
		b3	0.25	350	0.8	0.31
		b4	0.25	400	0.64	0.38

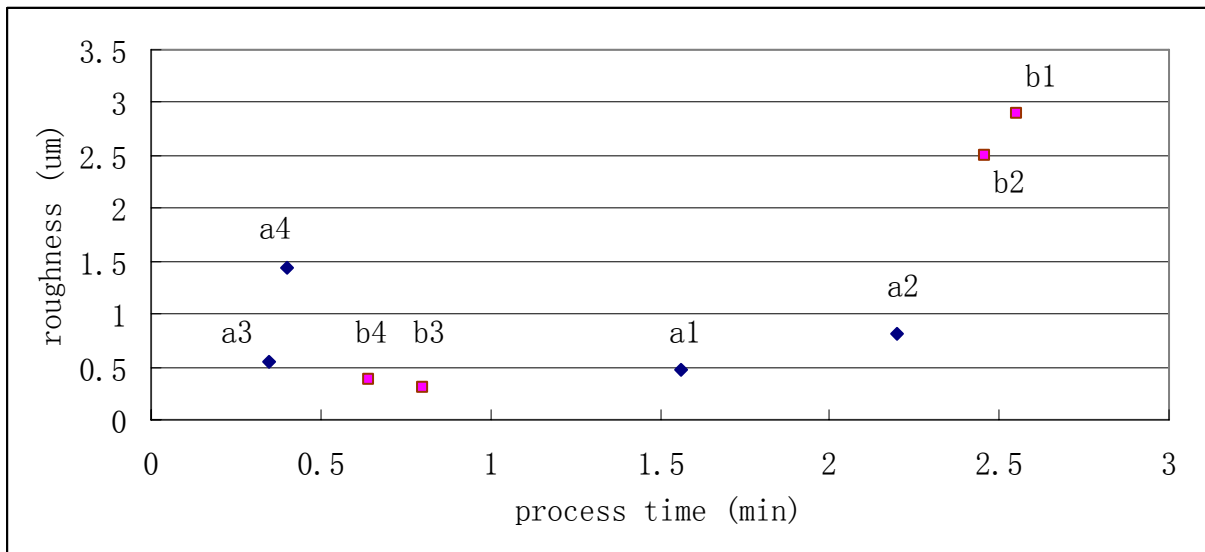
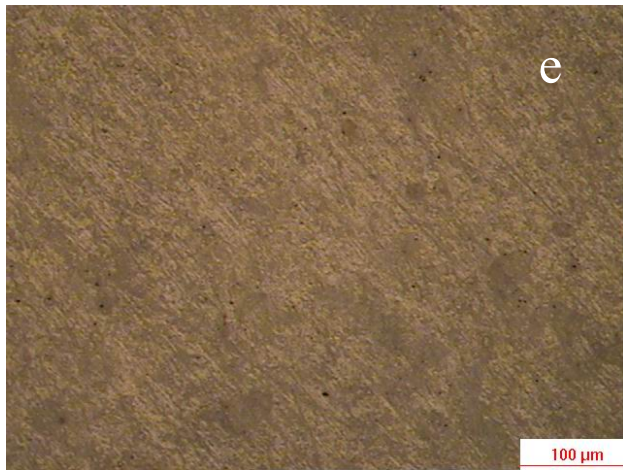
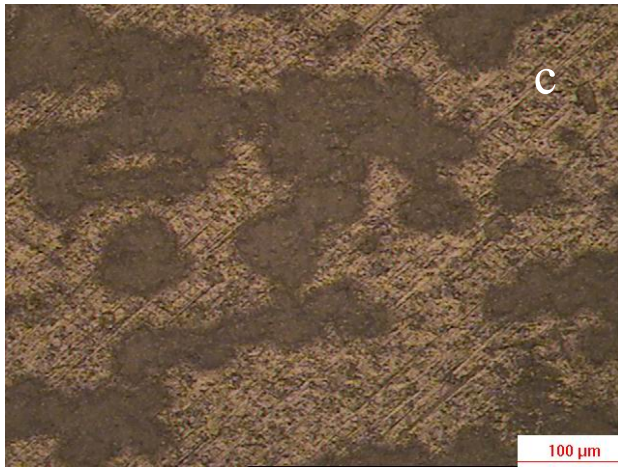
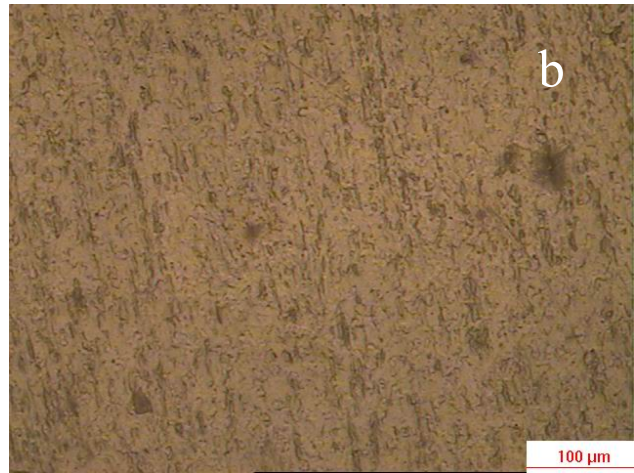
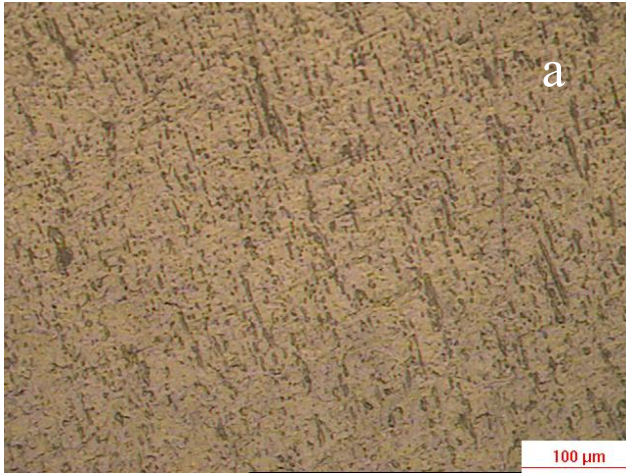


Figure 1 Roughness data of the PEO coatings vs process time

From Table 1 and Figure 1, we can clearly see that the samples with relative low current density took a much longer time (about four times as much) as the samples with higher current density to achieve the terminal voltages. Under the same process conditions (I and U), group B samples took longer time to achieve terminal voltage. The roughness of the coatings deposited on b3 and b4 were very high. This may be explained by with an increase in process time, stronger localized discharges on the surface of the coatings produced a rougher surface. According to the SEM micrographs (Figure 6) of the crosssectional view of the coating b1 and b2, we can also see a lot of cracks existed parallel to the metal/oxide boundary.

Optical micrographs in Figure 2 show the morphology of these coatings. The coatings of short processing time were comparatively compact, while the coatings of long processing time were rougher, and there were many micro-cracks on the surface of the coating. These porous surfaces showed that certain amount of oxide striped off from the coating. This fixed well with the statement in Ref.[7]



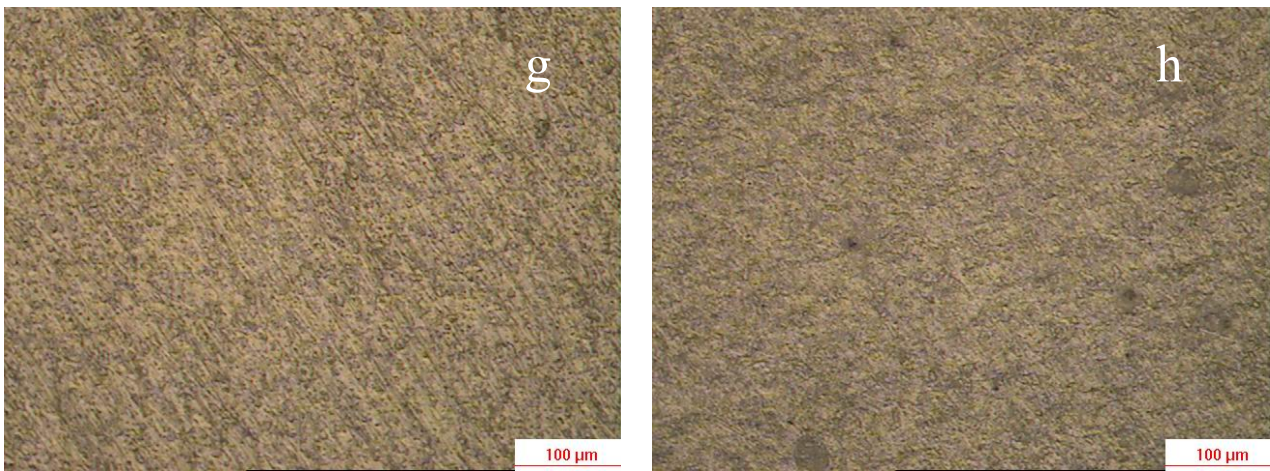


Figure 2 Optical micrographs showing the morphology of the PEO coatings of Group A (a, b, c, d) and Group B (e, f, g, h).

3.1 Corrosion tests

Figure 3 shows the polarization curves for the Zr substrate and coated samples prepared using the two concentration ratios of Na_2SiO_3 and KOH solutions and two current densities. According to the PEO experiments, the processing time and coating surface morphologies depend mostly on the current densities. The corrosion behaviour of the coatings a1, a3 deposited from 8g/l: 8g/l Na_2SiO_3 and KOH solutions b1 and b3 (see Table 1).

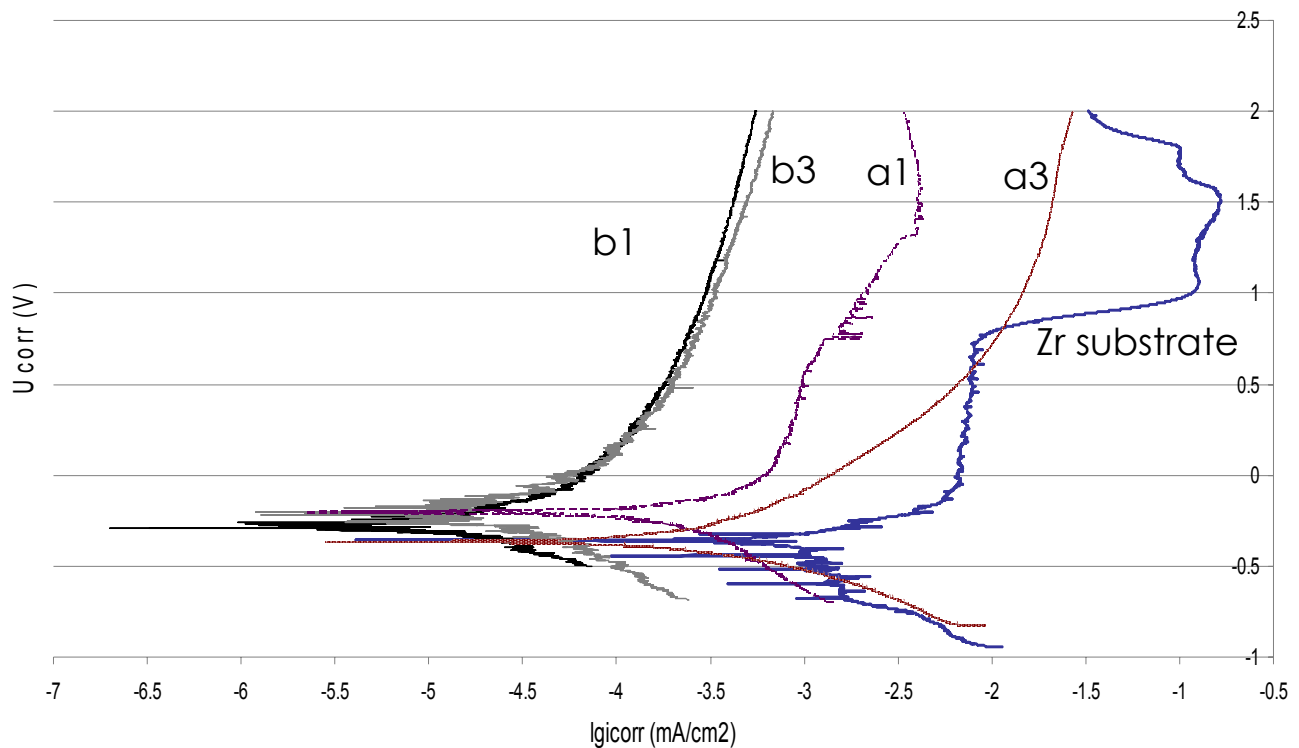


Figure 3 Potentiodynamic polarization curves of the uncoated Zr-2.5Nb and coatings deposited from sample a1 and a3 in 1:1 electrolyte and samples b1 and b3 in 10:1 electrolyte of Na₂SiO₃ and KOH.

The corrosion potentials, corrosion current density, and anodic/cathodic Tafel slopes (*b_a* and *b_c*) were obtained from test results. Then, based on the approximate linear polarization at the corrosion potential (*E_{corr}*), the polarization resistance(*R_p*) values were determined using the relationship[5, 10]:

$$R_p = \frac{b_a \times b_c}{2.3 \times i_{corr} (b_a + b_c)} \quad (1)$$

Where *i_{corr}* is the corrosion current density, *b_a* and *b_c* are the anodic/cathodic Tafel slopes.

A summary of the results of the potentiodynamic corrosion tests is given in Table 2. The data clearly show the enhanced corrosion protection afforded by the coatings. There were significant decreases in the *i_{corr}* of all the coated samples which showed a higher corrosion resistance than that of the zirconium substrate (more than one order of magnitude). The coatings of Group B (8g/l : 0.8g/l) had better corrosion resistance than that of Group A (8g/l : 8g/l), the relative low *R_p* of samples a3 and a4 might be explained by the short process time, which resulted in thin coatings, during the PEO process, this can also be seen by the crosssectional SEM micrographs of the coatings shown in part 3.4. From Table 2, we can also find that the corrosion potential (*E_{corr}*) of coated samples varied from -0.19 to -0.32V, all of which were higher than that of the Zr substrate (-0.33V).

Furthermore, from Figure 3, we can see that at a potential of about 0.78V, the current density suddenly increased by about two orders of magnitude for the uncoated sample. These may have resulted from the fact that the corrosion resistance considerably decreased after the thin protective oxide film on the uncoated substrate surface was broken down during the corrosion process. The large corrosion craters could also be clearly observed by naked eye on the surface of uncoated zirconium after corrosion testing (Figure 3).

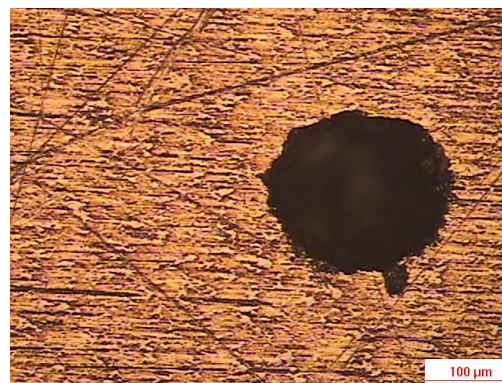


Figure 4 Optical micrograph of the corrosion crater of protective films on Zr substrate during corrosion process.

Table 2 Results of the potentiodynamic corrosion tests in a 0.4mol/L LiOH solution

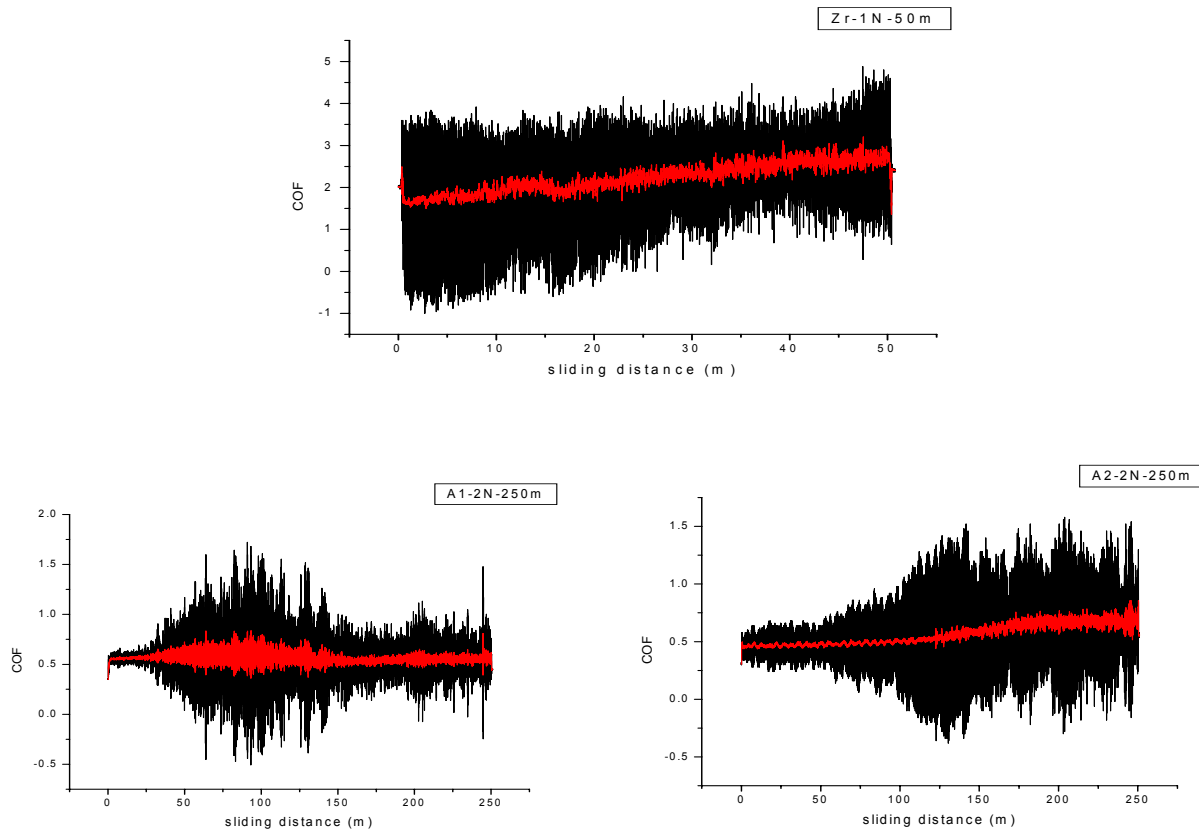
Samples	<i>i_{corr}</i> (mA/cm ²)	<i>E_{corr}</i> (V)	<i>R_p</i> (Ωcm ²)
Zr substrate	1.02E-3	-0.33	1.22E+4

a1(0.15A/cm ² ,350V)	7.08E-5	-0.19	1.15E+6
a2(0.15A/cm ² ,400V)	3.98E-5	-0.25	1.12E+6
a3(0.25A/cm ² ,350V)	1.99E-4	-0.32	2.16E+5
a4(0.25A/cm ² ,400V)	7.94E-5	-0.30	6.08E+5
b1(0.15A/cm ² ,350V)	6.31E-6	-0.27	5.78E+6
b2(0.15A/cm ² ,400V)	5.71E-6	-0.26	4.43E+6
b3(0.25A/cm ² ,350V)	1.58E-5	-0.21	3.25E+6
b4(0.25A/cm ² ,400V)	2.09E-5	-0.22	1.62E+6

3.3 Pin-on-disc tests

Tribological behaviour tests on coated and uncoated samples against Al₂O₃ pin balls as counterface materials under dry sliding condition. Figure 5 shows tribological behaviour of the various testing samples in the dry condition. Microcal Origin software was used to smooth the curves in order to get the values of coefficients of friction (COF) at a stable stage, which are listed in Table 4.

COF of the coatings of Group A varied greatly from each other. Coating a4 exhibited a low coefficient of friction (COF=0.22), while coating a1, a2 and a3 and showed a high COF (>0.5). In Group B, all the coatings had relative even COF. In Figure 6, relatively large amounts of coating material were lost on the wear track of coating a3 comparing to the coating a1, so the wear track of a3 showed to be deeper.



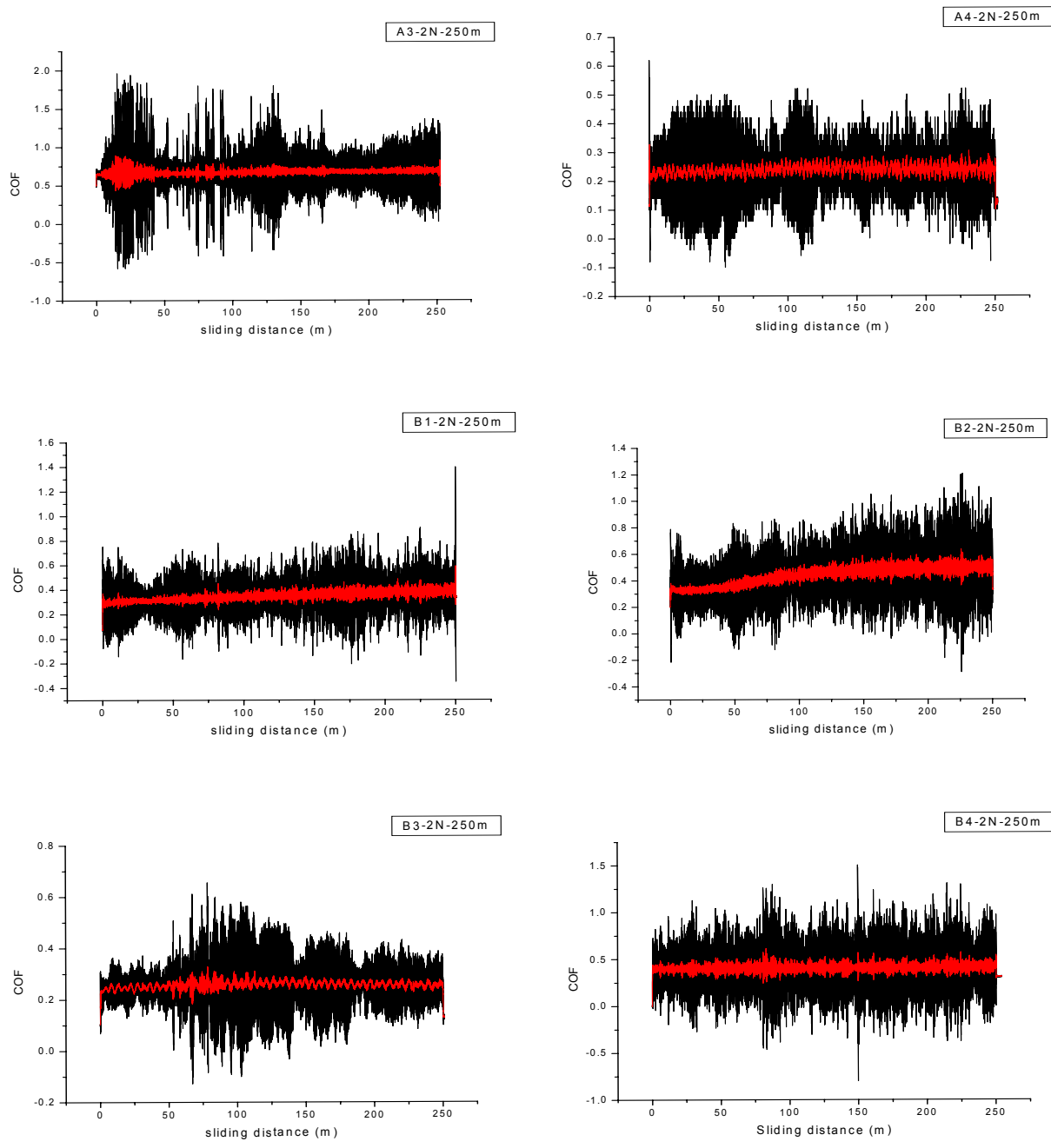


Figure 5 Tribological behaviours and the COF of uncoated/coated samples against Al_2O_3 pins.

Table 4 COF of the uncoated and coated samples

Samples	Zr substrate	a1	a2	a3	a4	b1	b2	b3	b4
COF	1.8	0.5	0.5	0.7	0.22	0.3	0.35	0.35	0.4

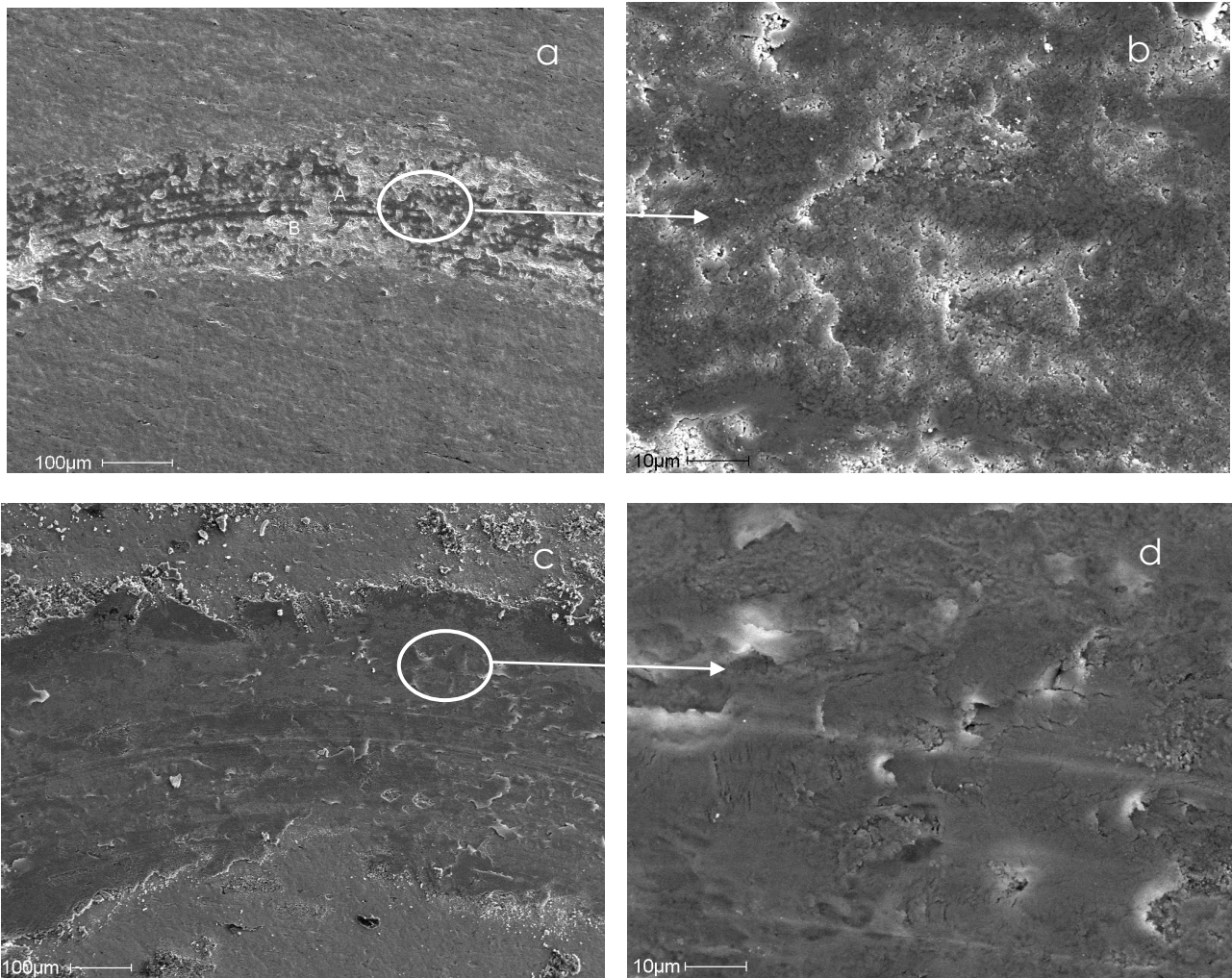


Figure 6 SEM micrographs of wear tracks on samples a1 (a and b) a3 (c and d) at different magnifications

3.4 SEM and EDS analyses

Figure 7 shows the crosssectional SEM micrographs of the sample a3 and b2. The results of the potentiodynamic corrosion tests tell that the sample a3 had the lowest polarization resistance (R_p) and in the SEM micrographs, it appeared to be lowest in thickness (about 2.5-3 μm) and the sample b1 and b2, which had highest roughness also had highest thickness. Samples b1 and b2 also showed better corrosion resistance (R_p) during the corrosion test (Table 2). Other samples showed almost the same thickness (about 5 μm).

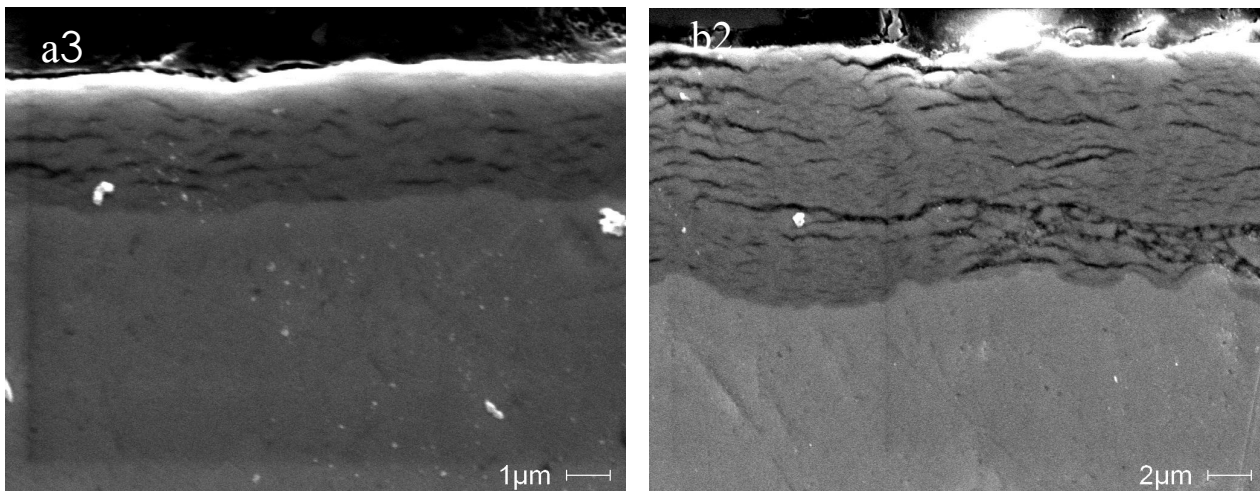
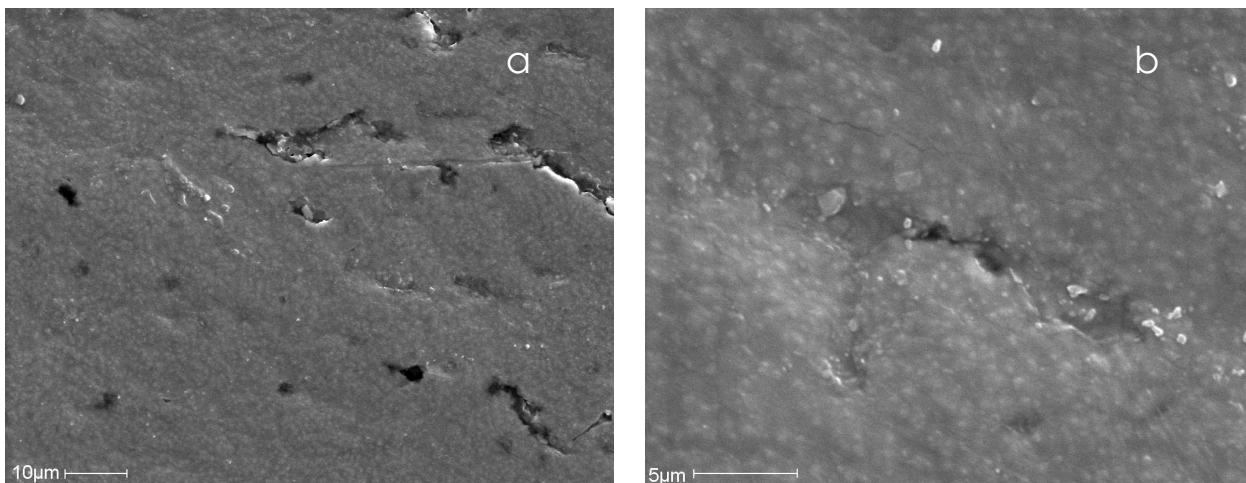


Figure 7 SEM micrographs of cross-sectional view of the PEO coatings (a3 and b2) at different magnifications

According to Table 1, the process time of the PEO coating depends mainly on current density. The coatings which deposited under high current density and short processing time had grey, smooth surfaces, however, the coatings which deposited under low current density and longer processing time had relative white and pitted surfaces. The SEM image of the coating deposit under low current density exhibits a morphology quite different from that of the high current density. For sample a1, which has low current density and longer treatment time had many micro-holes which distributed over the surface of the coating (Figure 8 (a and b)). Some cracks formed after corrosion (Figure 8 (c and d)). For sample a3, which has higher current density and short treatment time showed a relative smooth surface under SEM. But after corrosion, some coral-like structures (Figure 9) formed in the corroded areas which exhibited dark areas on optical micrographs. EDS spectra collected from these dark areas shows the chemical composition.



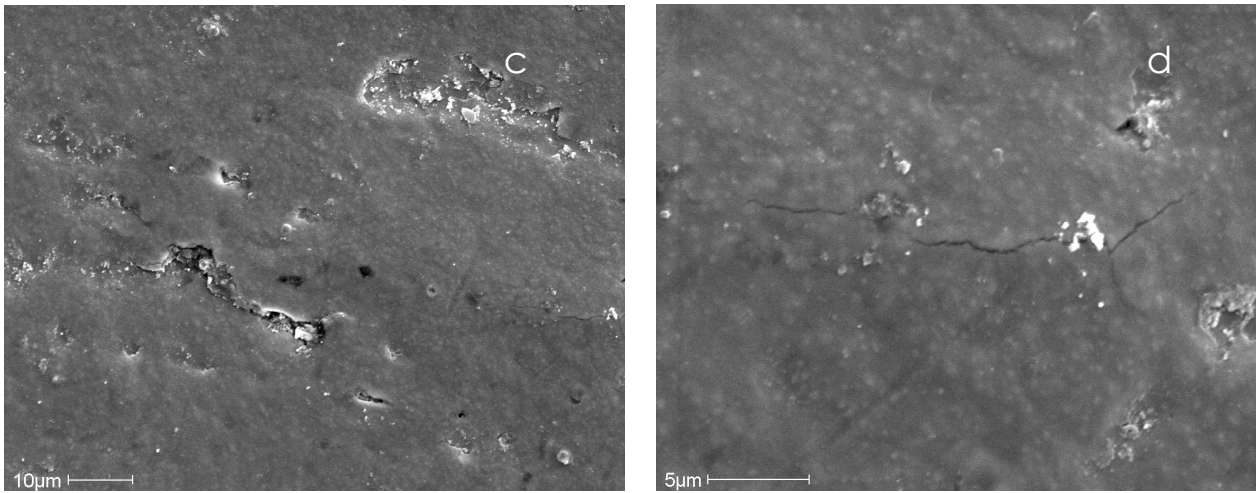


Figure 8 SEM micrographs of morphology on sample a1 (a and b) before and (c and d) after corrosion at different magnifications

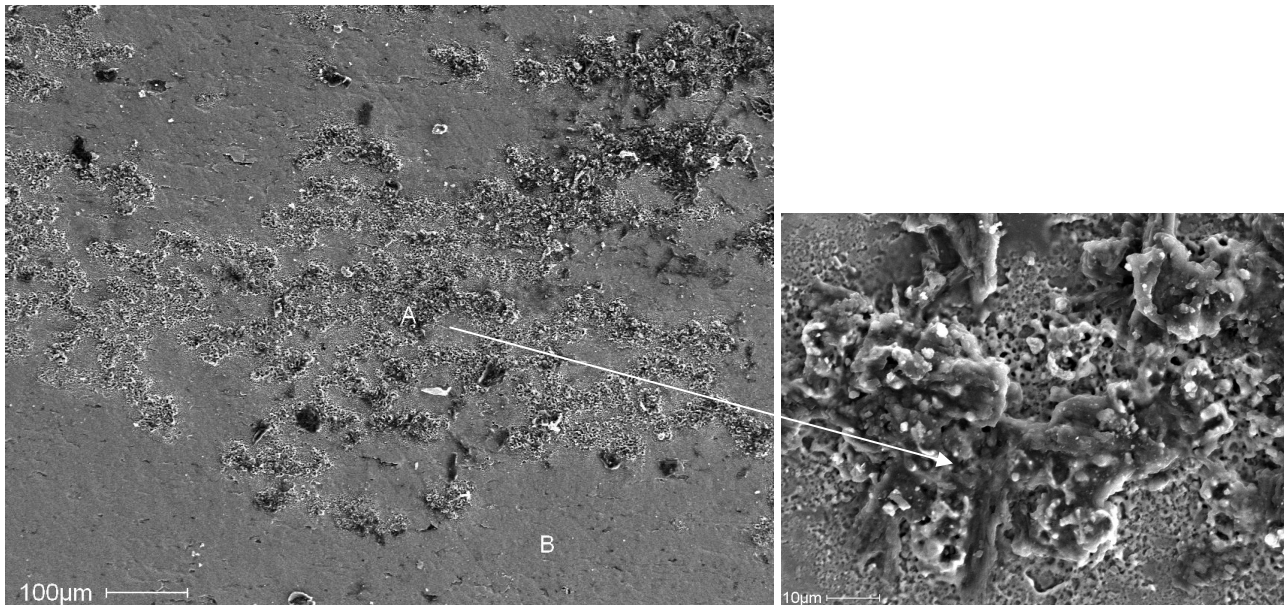


Figure 9 SEM micrographs of morphology on sample a3 after corrosion

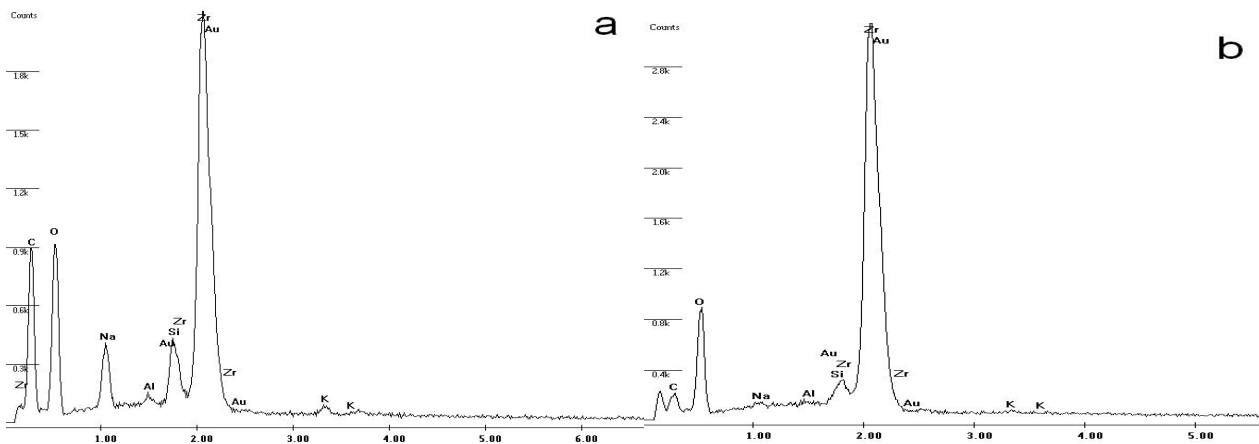


Figure 10 EDS spectra collected from corroded coatings of sample a3 on (a) dark A areas and (b) bright B areas.

4. Conclusions

The PEO coating deposited on Zr-2.5Nb in alkaline electrolytes greatly improve the corrosion resistance in the LiOH alkali solution by more than 10 times enhancement in R_p . What's more, the coatings deposited in the solution of Na_2SiO_3 : KOH =10:1 showed higher corrosion resistance than that deposited in the electrolyte which had concentration ratio of 1:1. Coatings on Group B also had a much higher surface roughness R_a , which resulted from longer process time during PEO process and greater thickness of the coating—about 8 μm on average. However, the thick coating also had a lot of cracks inside which may bring forward strip-off of the outer layer of the coating and contaminate the coolant and even damage the tubes of the bundle.

5. Acknowledgements

The authors would like to thank Mr. John W. Robinson for his assistance in preparation SEM micrographs and EDS collection.

6. References

1. Kim, H., et al., "Evaluation of pre-transition oxide on Zr--0.4 Nb alloy by using the HVEM". *Journal of Nuclear Materials*, 2008. 374(1-2).
2. Meng, X. and D. Northwood. *Intermetallic Precipitates in Zirconium--Niobium Alloys*. 1988: ASTM International.
3. Northwood, D., X. Meng-Burany, and B. Warr. *Microstructure of Zr--2. 5 Nb Alloy Pressure Tubing*. 1990: ASTM International.
4. A. L. Yerokhin, X. Nie, A. Leyland, A. Matthews, S. J. Dowey. "Plasma electrolysis for surface engineering" *Surface & Coatings Technology*, 1999. 122(2-3): p. 73-93.
5. Y. Ma, X. Nie, D.O. Northwood, H. Hu. "Corrosion and erosion properties of silicate and phosphate coatings on magnesium". *Thin Solid Films*, 2004. 469: p. 472-477.
6. Yong-jun, G. and X. Yuan, "Review on plasma electrolytic deposition. *Advances in Mechanics*", 2004. 35(2): p. 237-250.
7. Z. P. Yao, Y. L. Jiang, Z. H. Jiang, F. P. Wang, Z. D. Wu. "Preparation and structure of ceramic coatings containing zirconium oxide on Ti alloy by plasma electrolytic oxidation". *Journal of Materials Processing Tech.*, 2008. 205(1-3): p. 303-307.
8. Klapkiv, M., N. Povstyana, and H. Nykyforchyn, "Production of conversion oxide-ceramic coatings on zirconium and titanium alloys". *Materials Science*, 2006. 42(2): p. 277-286.

9. Y. H. Jeong, J. H. Baek, S. J. Kim, H. G. Kim, H. Ruhmann. "Corrosion characteristics and oxide microstructures of Zircaloy-4 in aqueous alkali hydroxide solutions". *Journal of Nuclear Materials*, 1999. 270(3): p. 322-333.
10. Jones, D., "Principles and Prevention of Corrosion." Macmillan Publishing Company, 866 Third Ave, New York, New York 10022, USA, 1992. 568, 1992.